Journal of Pharmaceutical Sciences 110 (2021) 2562-2569

Contents lists available at ScienceDirect

Journal of Pharmaceutical Sciences

journal homepage: www.jpharmsci.org

Pharmacokinetics, Pharmacodynamics and Drug Transport and Metabolism

Predicting Oral Absorption for Compounds Outside the Rule of Five Property Space

Felix Huth [a, *], Norbert Domange [a], Birk Poller [a], Arpine Vapurcuyan [b], Alexandre Durrwell [a], Imad D. Hanna [c], Bernard Faller [a]

[a] Pharmacokinetic Sciences, Novartis Institutes for BioMedical Research, Basel, Switzerland
[b] Regeneron Pharmaceuticals, Tarrytown, NY, USA
[c] Pharmacokinetic Sciences, Novartis Institutes for BioMedical Research, East Hanover, NJ, USA

ARTICLE INFO

Article history:
Received 14 December 2020
Revised 20 January 2021
Accepted 28 January 2021
Available online 1 February 2021

Keywords:
Permeability
MDCK
Fraction absorbed
Lipophilic compounds
BSA
Lysosomal trapping
P-gp knockout

ABSTRACT

The estimation of the extent of absorption of drug candidates intended for oral drug delivery is an important selection criteria in drug discovery. The use of cell-based transwell assays examining flux across cell-monolayers (e.g., Caco-2 or MDCK cells) usually provide satisfactory predictions of the extent of absorption in vivo. These predictions often fall short of expection for molecules outside the traditional low molecular weight property space. In this manuscript the transwell permeability assay was modified to circumvent potential issues that can be encountered when evaluating the aforementioned drug molecules. Particularly, the addition of albumin in the acceptor compartment to reduce potential binding to cells and the acceptor compartment, improved the predictive power of the assay. Cellular binding and lysosomal trapping effects are significantly reduced for larger molecules, particularly lipophilic bases under these more physiological conditions, resulting in higher recovery values and a better prediction power. The data indicate that lysosomal trapping does not impact the rate of absorption of lipophilic bases in general but is rather an exception. Finally, compounds believed to permeate by passive mechanisms were used in a calibration curve for the effective prediction of the fraction absorbed of molecules of interest in current medicinal chemistry efforts.

Introduction

Oral drug delivery is the preferred and most convenient option for the administration of therapeutic agents to patients. Naturally, early drug discovery programs incorporate permeability and solubility considerations into the medicinal chemistry decision tree on top of features required for potency. Optimization of these two critical parameters (i.e., solubility and permeability) improves the probability for sufficient systemic exposure and tissue concentrations that are required for efficacy. When solubility is not rate-limiting at the therapeutic dose, the fraction absorbed is largely dependent on the permeability through the intestinal wall of the gastro-intestinal (GI) tract. Multiple *in vitro* assays have been proposed to predict GI permeability, including measurement of octanol/water partition coefficients, parallel artificial membrane permeability assay (PAMPA), cell-based assays using Caco-2 or Madin-Darby Canine Kidney (MDCK) cell monolayers or intestinal tissue mounted in an Ussing chamber. Alternatively permeability may be predicted using in silico models.[1,2] *In vitro,* permeability is typically measured in a transwell setup, where the rate and extent of permeation across a monolayer of epithelical cells such as Caco-2 grown on semipermeable membranes are estimated. Caco-2 cell monolayers owing to their heterogeneous nature in their expression of potentially interfering uptake and efflux transporters, may not be the best *in vitro* model to determine the passive permeability.[3] Instead, many laboratories use a selected subclone derived from wild-type Caco-2 cells (C2BBE1) and subsequently eliminated the expression of selected efflux transporters by genetic knockout to overcome the heterogeneity and interfering efflux activity.[4] Alternatively, MDCK cell sub-clones with low efflux transporter activity (MDCK-LE) can be used to enable determination of passive permeability.[5,6]

Current biological target(s) engagement strategies have necessitated the expansion of the chemical space typically employed in

Conflicts of Interest: F.H., N.D., B.P., A.D., I.D.H. and B.F. are employees of Novartis Institutes for BioMedical Research; N.V. was an employee of Novartis Institutes for BioMedical Research; All other authors declared no competing interests for this work. All authors, except A.D. are stock owners of Novartis shares.
Research data used in preparation of this manuscript is available, contact the corresponding author.

* Corresponding author. Fabrikstrasse 14, 4002 Basel, Switzerland.
E-mail address: felix.huth@novartis.com (F. Huth).

https://doi.org/10.1016/j.xphs.2021.01.029
0022-3549/

existing pharmaceutical agents. The resulting drug molecules, referred to as beyond rule of five agents,[7] have chemical properties that impose special challenges on the traditional drug delivery approaches and absorption assessment investigations. For example, disrupting protein-protein interactions or targeted protein degradation typically require molecular weight values higher than the majority of generic drugs. An increasing number of molecules in early discovery have a molecular weight beyond 500 Da, increased lipophilicity and a higher number of hydrogen bond donors and acceptors. The current transwell permeability screening assay protocols were designed and validated with molecules within the rule of five property space, and often with a limited training set made of small hydrophilic and small hydrophobic molecules. With time, it became clear that the screening protocol led to an increased number of compounds with under-predicted Fa compared to the observed bioavailability in human and in rat at low dose (Table 1). The incidence of poor recovery (<30%) was also increasing, leading to a higher fraction of compounds annotated as undefined. Multiple effects may explain the under-estimated permeability, such as binding to labware, binding to cells, lysosomal trapping, P-glycoprotein (P-gp) mediated efflux and instability of the compounds. Lysosomal trapping can lead to increased cellular concentrations, potentially resulting in a depletion of the investigated compound. In order to prevent this effect, bafilomycin A1, an inhibitor of the H/K-ATPase, can be added.[8,9] In vivo lysosomal trapping is suspected to delay absorption.[10] Cellular binding and plastic binding can be reduced by adding bovine serum albumin (BSA) to the acceptor compartment as described by Saha & Kou.[11] Chemical instability can be assessed in a separate assay. The permeability of low molecular weight compounds (MW: $\leq$ 300 g/mol) derived from Caco-2 or MDCK-LE assays are known to under-predict Fa due to a too tight cell monolayer, not well reflecting the in vivo paracellular pathway.[12] In order to account for paracellular transport a mathematical correction can be applied to permeability results as described by Adson et al. and Sugano et al.[13,14]

This work was triggered by the large disconnect observed between the poor permeability measured for fingolimod, siponimod, eltrombopag, amiodarone and one additional internal compound using the conventional MDCK assay (V1) while these compounds were well absorbed orally in human or rat (Table 1). In this investigation the effects of bafilomycin A1 and BSA on transwell permeability are described. The objective of this study was to establish a new calibration of permeability versus Fa with optimized MDCK assay conditions (V2) accounting for the more lipophilic chemical space.

Material and Methods

Chemicals

Except for Novartis compounds (in-house synthesis), all compounds were purchased from Sigma-Aldrich and dissolved in DMSO at a final concentration of 10 mM. Novartis in-house compounds were randomly selected, lipophilic compounds and calibrator were selected based on availablility of in-house or published Fa data.

Cell Culture and Permeability Assay Conditions

To determine the apparent permeability (Papp), MDCK-low efflux (MDCK-LE clone E_9) or MDCK knockout (MDCK-KO) cells were seeded on Transwell 96-well plate inserts (Corning, Tewksbury, MA, Supplementary Table S1) at a density of 1.5×10^5 cells/cm^2 in high glucose DMEMwith GlutaMAX containing 10% v/v heat

Table 1
BSA Concentration-Dependent Impact on Apparent Permeability.

Compound	BSA Concentration in Acceptor (%)	Papp (10^{-6} cm/s)	Recovery (%)	Human Fraction Absorbed (%)
Siponimod	0.1	1.39 ± 0.093	73 ± 0.128	>90[a]
	1	10.5 ± 0.690	68 ± 0.947	
	5	24.3 ± 3.31	85 ± 4.54	
	10	27.9 ± 5.53	89 ± 7.59	
	20	25.5 ± 3.10	87 ± 4.25	
Fingolimod	0.1	0.490 ± 0.014	24 ± 0.019	>93[a]
	1	2.47 ± 0.080	24 ± 0.110	
	5	7.07 ± 1.08	36 ± 1.48	
	10	13.1 ± 1.79	40 ± 2.46	
	20	7.62 ± 0.734	37 ± 1.01	
Rifampicin	0.02	3.16 ± 0.164	100 ± 0.262	>93[a]
	1	3.26 ± 0.109	86 ± 0.150	
	2.5	3.23 ± 0.264	87 ± 0.362	
	5	3.52 ± 0.301	84 ± 0.413	
	10	3.56 ± 0.090	93 ± 0.124	
Amiodarone	0.1	0.122 ± 0.010	12 ± 1.00	50[a]
	1	0.370 ± 0.006	41 ± 0.577	
	5	1.73 ± 0.308	36 ± 0.422	
	10	3.09 ± 0.760	40 ± 1.04	
	20	1.71 ± 0.338	36 ± 0.465	
Eltrombopag	0.1	4.69 ± 0.022	79 ± 0.738	≥52[b]
	1	9.40 ± 1.39	85 ± 1.91	
	5	15.2 ± 1.03	96 ± 1.42	
	10	19.6 ± 1.52	95 ± 2.09	
	20	13.5 ± 1.57	86 ± 2.16	
NVP100	0.02	0.081 ± 0.007	39 ± 0.477	100[c]
	1	2.15 ± 0.043	64 ± 0.059	
	2.5	4.19 ± 0.204	71 ± 0.280	
	5	10.8 ± 1.21	70 ± 1.66	
	10	15.6 ± 0.937	75 ± 1.29	

[a] Fa references in Supplementary Table S3.
[b] Eltrombopag, EU Summary of Product Characteristics.
[c] Bioavailability in the rat, data on file.

deactivated FBS and 1% v/v penicillin-streptomycin (all from Gibco) and grown for 4 days at 37 °C in an atmosphere of 5% CO_2 and 95% relative humidity. Stock solutions of the compounds were prepared in dimethyl sulfoxide (DMSO) (10 mM), and each compound was dosed in triplicate at a final concentration of 10 μM in Hanks' balanced salt solution (HBSS) at pH 7.4 containing 10 mM HEPES and 0.02% w/v bovine serum albumin (BSA) using the historic method (MDCK-V1). Applying the new method (MDCK-V2), 0.02% BSA were added to the donor compartment and 5% BSA to the acceptor. Bafilomycin (100 nM) was added to both compartments. Cells were incubated with the compounds for 2 h at 37 °C, and flux was measured in the apical-to-basolateral direction. Dosing solutions as well as the calibration solutions were centrifuged for 60 min at 4000 g at 4 °C for protein precipitation. Drug concentrations in the donor and acceptor compartments were measured by liquid chromatography−mass spectrometry (LC-MS), using a six-point calibration curve, glyburide as an analytical internal standard. Trapping effects of lipophilic bases: The impact of lysosomal trapping on apparent permeability and recovery was investigated by an experiment with the MDCK-V2 assay without and with bafilomycin A1. Increased lipophic conditions in the acceptor compartment: to determine if increased lipophilic conditions in the acceptor compartement can further reduce cellular binding and increase apparent permeability, the donor and acceptor buffer of the MDCK-V2 assay were varied: 0.02% BSA, 4% BSA or 0.02% BSA +200 μM maisine (a pharmaceutical oily vehicle derived from corn oil containing linoleic mono-, di- and triglycerides) for the donor and 5% BSA or 5% BSA + liposomes (20 mg/mL egg lecithin) for the acceptor. Cellular trapping and nonspecific binding in the acceptor compartment: The compounds siponimod, eltrombopag and quinacrine were incubated under conditions of the MDCK-V1 and −V2 assay. At the end of the experiment the amount of compound in the three compartments, donor, acceptor and cells, was determined by LCMS quantification. LC-MS Method: Phenomenex Kinetex Polar C18 column, 30*2.1 mm, 2.6 μm; oven temperature: 50 °C; injection volume: 1 μL; mobile phase A: water containing 0.1% (v/v) formic acid, mobile Phase B:acetonitrile containing 0.1% (v/v) formic acid and 4% (v/v) water, flow rate 0.8 mL/min; gradient: 2% B for 0.2 min, ramp up to 60% B in 0.8 min, ramp up to 100% B in 0.3 min and keep for 0.4 min, back to 2% B in 0.01 min and keep for 0.24 min. MSMS parameters, SCIEX QTRAP5500 using an ESI source, IonSpray Voltage: 4500 V (−4500 V in negative mode), Ion source Gas1: 60 psi, Ion source Gas2: 40 psi, Temperature: 450 °C, Curtain Gas: 30 psi, Collision Gas: 9 psi. All compound parameters such as parent mass, product mass, DP and others were obtained using the auto-tuning step of the DiscoveryQuant application. The scan time is 0.025 s. Protein quantification: DC protein assay kit, Biorad (# 500-0116).

Calculations of Physicochemical Properties

LogD7.4 values were determined as described by Low et al.[15] Topological polar surface area (tPSA) was calculated as described by Ertl et al.[16] ClogP values were computed using CLOGP Daylight Version 4.9 (http://www.daylight.com/dayhtml/doc/clogp/; BioByte, Claremont, CA).

Generation of the MDCK-KO Cell Line

MDCK wild type cells were used to generate a new cell line completely devoid of P-gp activity expression. The first step consisted in a functional sub-cloning of cells with a low P-gp mediated efflux activity using two sequential approaches. The MDCK-wild type cells (10×10^6/mL) were loaded as a suspension with Calcein-AM (#C3100MP Life Technologies) at a final concentration of 25 μM, for 45 min at 37 °C. The cells were washed 1× with HBSS and re-suspended in HBSS at a final cell concentration of 10×10^6/mL. FACS sorted cells with the highest fluorescence intensity were transferred in a sterile 96 well plate at an average of 1 cell per well and cultured until confluence. A second cycle was performed to select out the cells with the lowest efflux activity. To that aim, cells in the 96 well plate were loaded again with Calcein-AM and the cell clone showing the highest fluorescence intenstity was selected (clone E9) and further propagated and expanded into larger tissue culture flasks (0.3 cm^2–175 cm^2). In a second step a functional selection based on quinidine efflux ratio was performed. The MDCK-LE cells (~10^9) were diluted to 100 cells/ml and distributed in a 96 well plate at an average of 1 cell/well and cultivated until confluence. A single clone (E9-1) was selected based on its low efflux ratio with quinidine loaded at 10 μM on the apical side as a substrate and a large stock of clone E9-1 was produced and stored in liquid nitrogen.

The sub-clone E_9 was then used to knock out the residual canine P-gp activity. Guide RNAs (gRNA) targeting canine genomic P-glycoprotein exon 4 and exon 13 were designed based on the public genomic sequence data for canine P-gp exons 4 and 13. The final sequences of the guide RNAs used to target canine P-gp exon were gRNA 1: GCTATTCAAATTGGCTTGAT, gRNA2: GATAGGTTGTATATGTTGGT, gRNA3: TGCACTCCCTCTCATGATGC. Primers were designed to be optimally situated upstream of the target mutation site (shown in red) that upon successful targeting would result in the generation of a premature termination TAA codon. Each of the three primers preceded a proto-spacer adjacent motif sequence (PAM; 5′-NGG-3′) as shown in the yellow highlighted text. A similar approach was used to design targeting guide RNAs for exon 13.

MDCK-KO cells were plated into 6-well plates (~3×10^5 cells) and cultured overnight in humidified tissue culture incubator in DMEM medium supplemented with 10% fetal bovine serum (FBS) and 1% benzylpenicillin/dihydrostreptomycin. The following day each of the gRNAs (cloned into the targeting vectors containing the gRNA scaffold and the CAS9 cDNA) along with the donor vector plasmid (contains the puromycin selection marker) were transfected into the cells using the turbofectamine 8.0 reagent. Briefly, each of the gRNA plasmids (1 μg) was diluted into 250 μL Opti-MEM buffer along with 1 μg of the donor vector followed by the addition of 6 μL of the concentrated turbofectamine reagent. The mixture was gently mixed by pipetting and incubated for 15 min at room temperature. Cells were washed with PBS buffer and a fresh aliquot (~2 mL) of culture medium added to the cells. The individual Turbofectamine-containing tubes were added to labeled wells in a drop-wise fashion and the plates gently rocked to allow for efficient mixing. Cells were placed in the incubator and passaged (approximately 8 times) every 3 days. At each passaging, the cells were diluted at a 1:10 ratio with fresh medium. On approximately day 23 post the initial transfection, the antibiotic puromycin at a final concentration of 2.5 μg/mL was introduced to select for the cells that incorporated the puromycin resistance marker. The final concentration of puromycin used in this study was determined by running a puromycin "kill curve" which is the lowest dose required to completely kill non-transfected MDCK-LE cells in 4–7 days after its introduction. Cells that survived the puromycin selection (heterogeneous pool derived from multiple clones) were expanded and assayed for the elimination of the residual P-gp efflux activity in the MDCK-LE cells. Subsequently, single cell colonies (clonal selection) derived from individual cells were assayed for the lack of efflux activity and expanded for cryo-preservation and downstream studies (MDCK-KO). MDCK-KO cells were cultured on 24-well

transwell plates for 1 week and the bidirectional [^{3}H]digoxin permeability was examined.

Calculations

The apparent permeability (P_{app}) was calculated using Equation (1),

$$P_{app} = \frac{dQ}{dt} * \frac{1}{C_o} * \frac{1}{A} \quad (1)$$

with dQ being the amount of drug in the acceptor compartment, dt the assay time, C_0 the initial drug concentration and A the filter surface area. The non-linear regression analysis of the average P_{app} values versus human Fa was performed using the hyperbolic Emax model in Equation (2),

$$Fa = \frac{Fa_{max} * P_{app}}{K_{half} + P_{app}} \quad (2)$$

with K_{half} being the apparent permeability where a Fa of 50% is reached.

Results

Characterization of the MDCK-KO Cell Line

The P-gp mediated efflux leading to a lower permeability value of moderately permeable molecules was resolved by knocking out the residual canine P-gp activity still present in the low efflux MDCK clone (Fig. 1). The elimination of residual P-gp efflux activity was observed with only 1 of the 6 gRNAs that were tested. No P-gp mediated digoxin efflux was observed in MDCK-LE cells that were targeted with gRNA exon 4–3 as indicated by the efflux ratio (ER) of 1.07 compared to an ER of 7.30 for the parental MDCK-LE cells (Fig. 1). None of the gRNA targeting exon 13 showed the elimination of P-gp efflux (e.g. exon 13–2 ER: 11.8). The heterogeneous culture derived from the selection with exon 4–3 was subsequently serially diluted to generate clones derived from single cells. As shown in Fig. 1, all single-cell derived clones that were propagated demonstrate the lack of digoxin efflux activity. The clone derived from the single-cell colony 3 was further expanded and used in all subsequent studies.

Transwell Permeability Dependence on BSA Concentration in the Acceptor

Papp values in A to B direction as well as recovery values of siponimod, fingolimod, eltrombopag amiodarone and NVP100 increased significantly with increasing BSA concentrations in the acceptor compartment. For fingolimod, amiodarone and eltrombopag Papp values declined when increasing BSA from 10% to 20%. This phenomen requires further clarification. One potential explanation would be an incomplete extraction of the compounds by protein precipitation with acetonitrile in the acceptor compartment with increasing amount of BSA. This hypothesis is supported by the fact that the effect of a declining Papp with 20% BSA was largest for the most lipophilic compounds listed in Table 1.

BSA Impact on Compartmental Distribution in Transwell Assay

Transwell experiments with siponimod, eltrombopag and quinacrine were performed to quantify the amount of compound in the donor, the cells, and the acceptor compartments and comparing the MDCK-V1 and –V2 assays, i.e. in absence and presence of 5% BSA in the acceptor and bafilomycin A1 in donor and acceptor (Fig. 2). For all three compounds the intra-cellular concentrations significantly decreased in the MDCK-V2 assay compared to the V1 assay, most pronounced for siponimod and quinacrine. Higher acceptor concentrations were observed for all three compounds reflected by the increased Papp values (Table 1, Supplementary Table S2). Higher donor concentrations of about 9–26% were observed for all three compounds. Total recovery values, including cellular bound compound, significantly increased with the V2 assay by 18–35% for the three compounds. Quantification of BSA in donor and acceptor at 0 min and after 120 min incubation in the assay demonstrated that the protein levels remained unchanged for each compartment.

Influence of Physicochemical Properties on Papp

For all compounds permeability was measured with either 0.02% or 5% BSA in the acceptor compartment, while bafilomycin (0.1 μM) was present in both compartments. The largest Papp increase was observed for low permeable compounds in the MDCK-V1 assay (Fig. 3a). Moreover, the lower the recovery in the MDCK-

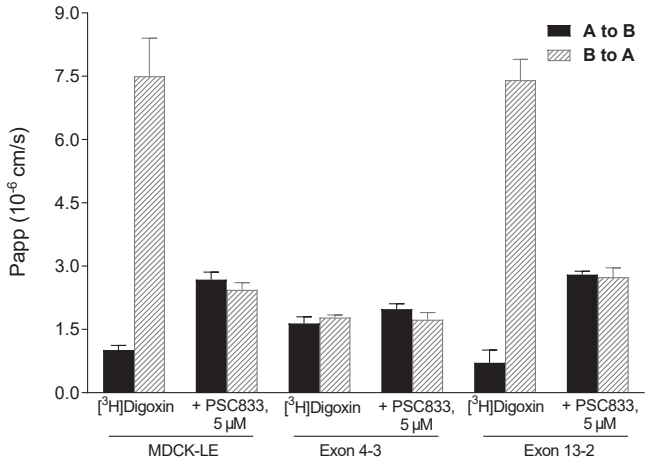

Fig. 1. Bidirectional transport of digoxin in the absence and presence of the P-gp inhibitor PSC833 for the cell lines MDCK-LE, MDCK-KO(exon 4–3) and MDCK-KO(exon 13–2).

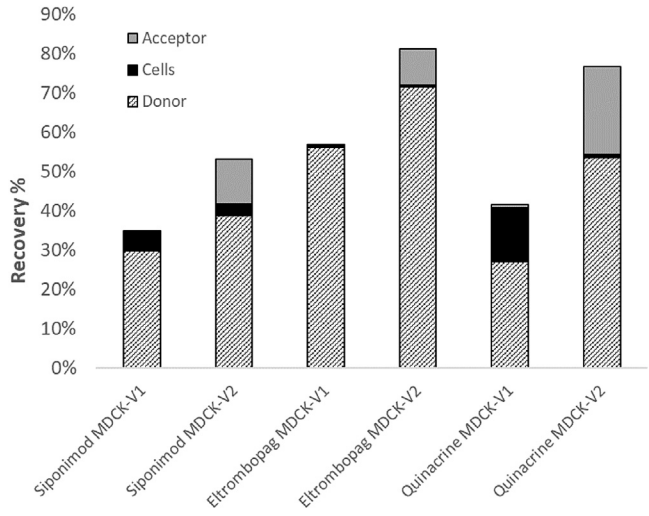

Fig. 2. Compartmental distribution of siponimod, eltrombopag and quinacrine after 120 min incubation with the MDCK-V1 and –V2 assay conditions.

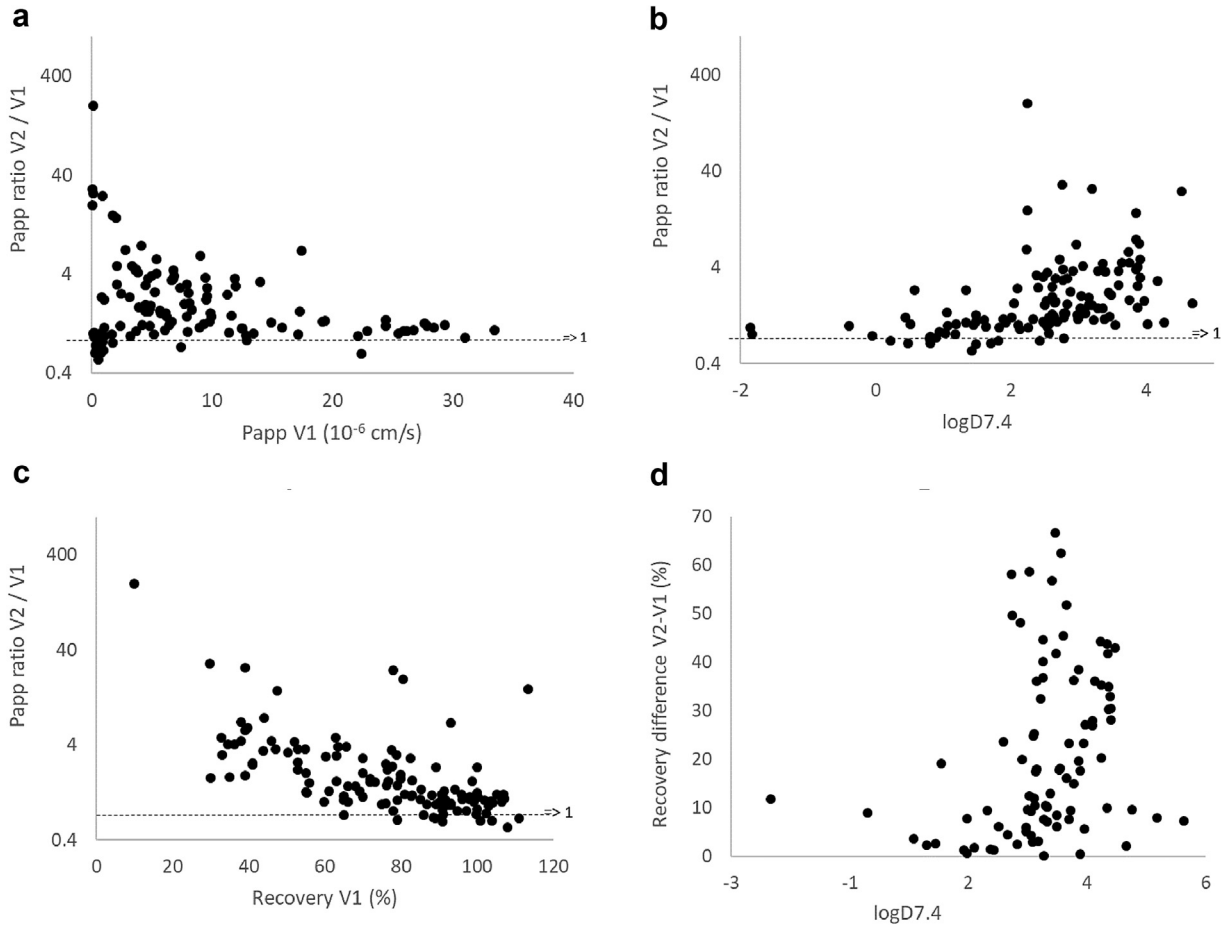

Fig. 3. Fold permeability increase (Papp ratio 5% BSA/0.02% BSA in acceptor) of Novartis research compounds versus Papp AB (0.02% BSA) (a), versus lipophilicity (logD7.4) (b) and versus recovery (0.02% BSA) (c); recovery difference between 5% and 0.02% BSA versus liphophilicity (d).

V1 assay, the higher the Papp value increased (Fig. 3c). Results were compared with the physicochemical properties, i.e. molecular weight, calculated logD(7.4) (clogD), polar surface area (PSA) (Supplementary Table S2). In general, with increasing lipophilicity Papp and recovery values increased in the V2 assay compared to V1 (Fig. 3b and d). For molecular weight and PSA no correlation was observed.

Impact of Bafilomycin A1

The impact on Papp of bafilomycin A1 in donor and acceptor in addition to 5% BSA in the acceptor was investigated for a set of compounds using the MDCK-KO cells (Fig. 4). For most of the compounds Papp values were within 2-fold deviation, with the exception of two compounds with a Papp below 1×10^{-6} cm/s (potentially due increased assay variability at for low Papp values) and quinacrine, fingolimod and amiodarone, which showed 5.4-, 2.9- and 3.5-fold higher Papp values in presence of bafilomycin A1, respectively (Supplementary Table S2).

Adding a Lipophilic Sink in the Acceptor Compartment

The addition of lecithin-based liposomes to the acceptor compartment on top of the 5% BSA substantially increased the apparent permeability of amiodarone to a Papp of 6.3×10^{-6} cm/s compared to the MDCK V2 conditions with a Papp value of 2.77×10^{-6} cm/s (Table 2). Addition of 5% BSA or 200 μM maisine (pharmaceutical oily vehicle derived from corn oil) in the donor resulted in a slightly decreased the Papp value. For NVP200 the Papp value was also increased when adding liposomes to the 5% BSA containing buffer in the acceptor. However, the addition of either 200 μM maisine or 4% BSA in the donor also resulted in a substantial increase of its apparent permeability. Recovery values for amiodarone and NVP200 were highest when adding liposomes to the acceptor compartment or 4% BSA to the donor compartment in addition to the MDCK V2 conditions.

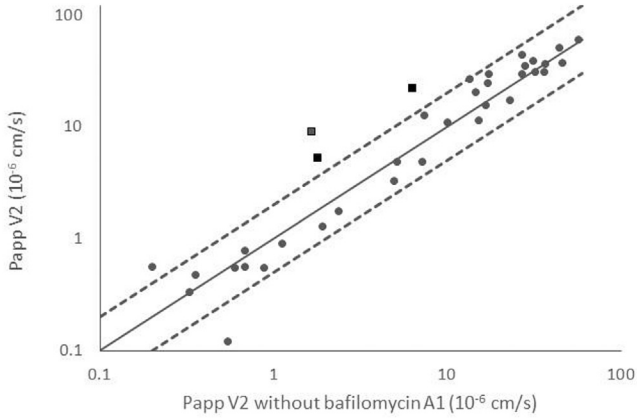

Fig. 4. Impact of bafilomycin A1 on apparent permeability.

Table 2
Impact of Different Buffers on Apparent Permeability on Lipophilic Compounds.

Compound	Donor Buffer	Acceptor Buffer	Papp (10^{-6} cm/s)	Recovery (%)
NVP200	0.02% BSA	5% BSA	1.18 ± 0.134	68.0 ± 0.184
	0.02% BSA + 200 μM Maisine	5% BSA	4.05 ± 0.200	64.8 ± 0.274
	4% BSA	5% BSA	4.72 ± 0.690	71.3 ± 0.947
	0.02% BSA	5% BSA + Liposomes	5.00 ± 0.121	88.6 ± 0.167
Amiodarone	0.02% BSA	5% BSA	2.66 ± 0.150	43.9 ± 2.96
	0.02% BSA + 200 μM Maisine	5% BSA	0.92 ± 0.007	40.0 ± 4.43
	4% BSA	5% BSA	1.78 ± 0.509	58.8 ± 1.40
	0.02% BSA	5% BSA + Liposomes	5.97 ± 0.382	57.2 ± 4.51

Calibration of Permeability Versus Fa

A set of calibration compounds was selected based on publications included in Supplementary Table S3. As the MDCK assay investigates passive permeability, compounds were carefully checked for absorption driven solely by passive transcellular permeability. Moreover, compounds with solubility limited absorption were discarded. Last, a consistency check of the published Fa values was done by comparing published clearance and bioavailability values. Considering all listed criteria, the initial list of 58 compounds was reduced to 39 compounds.

Three independent runs of the MDCK-V2 assay were performed with the calibrator compounds. The calculated mean Papp values and Fa were fitted applying Equation (2), resulting in a good coefficient of determination (R^2) of 0.956. The fitted values for Fa,max, K_{half} and the Hill coefficient were 100, 3.39 and 1.40, respectively (Table 3, Fig. 5). All compounds except erythromycin were within the 95% prediction band.

Discussion

Permeability is a key ADME parameter in drug discovery and development of orally delivered molecules. Therefore, it is important to determine this parameter with sufficient accuracy. The chemical space of recently developed drugs and of evolving

Table 3
Correlation Between Apparent Permeability (Papp AB) and Fraction Absorbed (Fa).

Compound	Fa (%)	MDCK-V1		MDCK-V2	
		Papp (10^{-6} cm/s)	Recovery (%)	Papp (10^{-6} cm/s)	Recovery (%)
Amiloride	50	2.72 + 0.111	89 + 0.152	3.18 + 0.686	94.0 + 5.57
Amiodarone	72	<0.2	31 + 2.32	2.66 + 0.150	44.2 + 2.96
Aztreonam	1	0.81 ± 0.173	96 ± 0.238	0.873 + 0.366	89 + 11
Benazepril	30	1.66 ± 0.034	92 ± 0.047	1.09 + 0.242	92.7 + 4.51
Carbamazepine	100	33.43 ± 4.24	98 ± 5.82	36.6 + 0.557	94 + 2
Cetirizine	60	5.14 ± 0.583	93 ± 0.801	5.34 + 0.342	93.7 + 1.53
Chloramphenicol	90	12.8 ± 0.418	100 ± 0.574	13.9 + 2.53	102 + 2.31
Clonidine	95	27.8 ± 2.75	94 ± 3.77	37.1 + 9.91	93.7 + 3.51
Clozapine	100	25.9 ± 6.56	85 ± 9.00	37.9 + 8.39	80.7 + 3.51
Daunorubicin	10	0.400 ± 0.092	77 ± 0.126	0.527 + 0.16	76.7 + 4.51
Diclofenac	99	22.9 ± 6.7	96 ± 9.20	43.5 + 2.64	90.3 + 3.06
Doxorubicin	5	0.310 ± 0.065	82 ± 6.58	0.463 + 0.015	93.7 + 3.79
Erythromycin	35	0.750 ± 0.070	91 ± 0.096	0.81 + 0.056	84 + 6.56
Fingolimod	95	0.120 ± 0.026	10 ± 0.036	15 + 2.87	44.7 + 9.81
Fluvastatin	100	12.8 ± 2.61	76 ± 3.58	17.3 + 2.79	81.7 + 9.71
Ganciclovir	3	0.980 ± 0.231	89 ± 0.317	0.543 + 0.055	92 + 3
Imatinib	98	17.4 ± 1.26	93 ± 1.73	30.8 + 3.95	96 + 7.21
Imipramine	100	24.4 ± 5.43	83 ± 7.45	45.7 + 7.99	93.7 + 3.79
Indinavir	63	5.38 ± 0.805	87 ± 1.10	7.25 + 1.22	89 + 7.94
Ketoconazole	95	13.5 ± 0.720	66 ± 0.989	30.7 + 2.32	70 + 12.2
Lamotrigine	100	31.0 ± 0.115	103 ± 0.158	32.8 + 1.16	96.7 + 2.08
Nicardipine	100	10.9 ± 0.575	54 ± 0.789	39.9 + 2.07	78 + 4
Olsalazine	3	0.410 ± 0.104	79 ± 6.64	1.04 + 0.441	93.7 + 10
Piroxicam	100	14.9 ± 2.78	62 ± 0.102	37 + 9.00	97.7 + 4.16
Prazosin	86	15.804 ± 1.87	65 ± 2.57	30.9 + 5.1	94 + 6.08
Progesterone	91	11.3 ± 3.06	39 ± 4.20	34.4 + 0.844	68 + 6.08
Propranolol	90	22.1 ± 2.52	75 ± 3.46	43.5 + 4.62	92 + 3
Propylthiouracil	90	19.6 ± 0.362	82 ± 0.497	21.7 + 0.478	83.3 + 0.577
Quinidine	95	27.6 ± 3.19	100 ± 4.38	33.3 + 8.33	97 + 4.36
Siponimod	90	0.150 ± 0.002	39 ± 0.003	12.4 + 1.98	52 + 12.1
Sulfadiazine	65	6.54 ± 1.56	87 ± 2.14	6.25 + 0.745	93.7 + 1.15
Sulfasalazine	13	0.980 ± 0.071	89 ± 0.098	1.18 + 0.128	86.7 + 2.52
Sulindac	90	7.23 ± 0.308	93 ± 0.422	7.45 + 0.627	91.3 + 4.16
Timolol	90	17.1 ± 0.145	104 ± 0.199	18.2 + 3.95	102 + 4.51
Tolbutamide	90	28.5 ± 4.82	100 ± 6.62	30.2 + 7.93	101 + 1.15
Verapamil	95	28.4 ± 3.25	98 ± 4.46	36.2 + 8.91	94.3 + 3.79
Viloxazine	99	27.8 ± 2.3	88 ± 3.16	41.6 + 12.1	98.7 + 3.21
Vinorelbin	27	1.56 ± 0.18	82 ± 0.20	1.56 + 0.18	82 + 0.20
Warfarin	98	26.2 ± 0.292	102 ± 0.401	42.6 + 2.12	103 + 3.06
low Fa threshold	20	0.148		1.18	
50% Fa	50	2.35		3.50	
high Fa threshold	85	14.3		12.5	

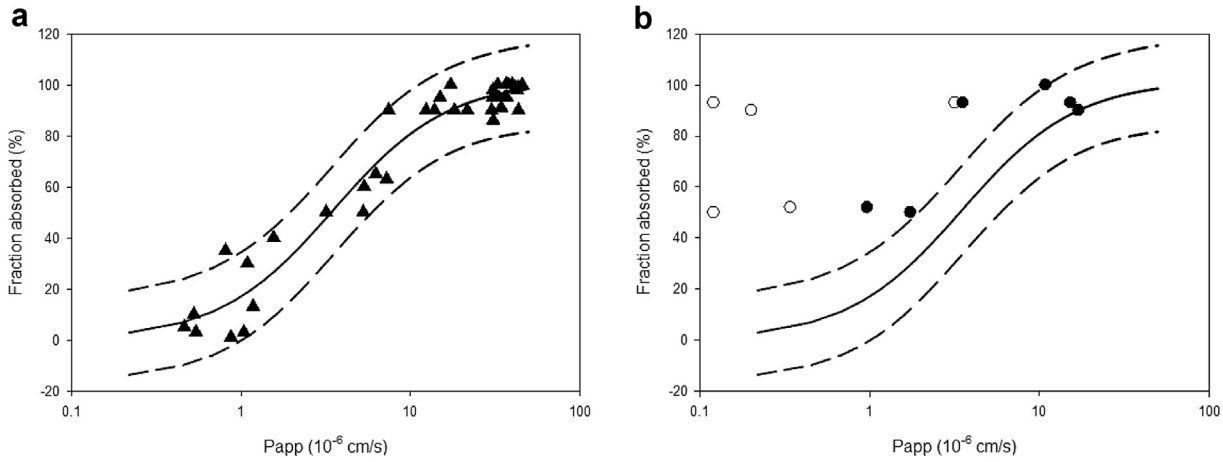

Fig. 5. Papp − Fa correlation for **a:** the set of calibrator compounds (closed triangles, Table 2) and b: for the set of beyond rule of 5 space compounds using MDCK-V1 (open circles) and V2 (closed circles, MDCK V1 and V2, Table 1). Solid and dashed lines represent the fitted correlation curve and the 95% prediction interval, respectively.

candidates goes beyond the rule of five, established by Lipinski in 1997.[7] Molecular properties move towards larger, more complex structures and compounds with higher lipophilicity. The development of an improved screening assay for transcellular permeability is one consequence to adapt to these recent changes.

Table 1 shows the concentration-dependent impact of BSA in the acceptor compartment on the apparent permeability of several lipophilic compounds. Although, the Papp values of siponimod, fingolimod and amiodarone were still increasing with higher BSA concentrations, 5% BSA was selected for the MDCK-V2 assay as a compromise between practical aspects and most optimal results. Fig. 5 displays the Papp shift of the lipophilic compounds when changing the assay conditions from V1 to V2, indicating a significantly improved correlation between Papp values and the observed fraction absorbed. The BSA concentration in the donor compartment was kept low (0.02%) to avoid reduced permeability of the compounds due to protein-binding effects. Investigating the permeability of compounds known to have a high binding to BSA, demonstrated no difference without BSA or 0.02% BSA (data on file). The low amount of protein also helps preventing non-specific binding and compound precipitation making high-throughput bioanalysis easier.

Quantification of siponimod, eltrombopag and quinacrine at the end of the incubation period of 120 min in the three compartments assay compartments, donor, cells and acceptor, demonstrated significantly reduced cellular concentrations with the V2 assay compared to the V1 conditions, especially for the highly lipophilic compound siponimod and quinacrine, a lipophilic diprotic base, which tends to be trapped in lysosomes. This reduced cellular to donor partitioning enabled a faster transition of molecules from donor to acceptor. Interestingly, not only the total recovery considering all three compartments increased, which might be explained by lower plastic binding in the acceptor, but also the donor recovery was substantially increased. The protein quantification at the end of the incubation revealed that there was no measurable change of protein levels in donor and acceptor, which might have explained the higher donor recovery.

The higher permeability values resulting from the addition of 5% BSA in the acceptor compartment may be explained by three reasons. First, plastic binding at low compound concentration in the acceptor compartment is reduced. Second, for highly permeable compounds which bind to BSA the assay will still be in sink conditions due to BSA binding, although more than 10% of the compound have migrated to the acceptor compartment within the assay time of 120 min. Third, lipophilic compounds tend to remain in the cell monolayer resulting in a high cellular partitioning (Kp, ratio of cellular to medium concentrations). Cellular accumulation is resulting in reduced donor concentrations which affects time for equilibration between unbound cellular and donor concentrations. Both effects reduce the apparent permeability. Adding BSA in the acceptor reduces the cellular Kp, enables a faster equilibration of unbound cytosolic concentrations and a lower reduction of donor concentrations due to cellular accumulation. The consequence of these redistribution processes is an increased Papp value observed for lipophilic compounds, resulting in more accurate Fa predictions. Moreover, the experimental condition with a protein gradient across the MDCK cell monolayer better reflects the intestinal/portal vein physiological conditions of the absorption process. The distribution process between cells and BSA in the basolateral compartment is affinity-driven. As shown in Table 1, Papp values increased with increasing BSA concentration. At high BSA concentration of 5−20% in the acceptor compartment Papp values reached a plateau for most compounds, although cellular concentrations were still high for certain compounds (i.e. fingolimod, amiodarone), indicated by low recovery values. In conclusion, the permeation process is not only controlled by diffusion but also by the relative binding affinity to cellular and basolateral compartment structures.

Bednarczyk and Shanghvi demonstrated that extensive lysosomal trapping affects Papp and recovery in transwell experiments.[8] In their work the MDCK-V1 protocol with 0.02% BSA in the dornor and acceptor was used. Interestingly, the impact lysosomal trapping was significantly reduced when 5% BSA was added to the acceptor compartment. Most of the lipophilic bases in Supplementary Table S2, e.g. propranolol, imatinib, imipramine, did not show a significantly increased Papp or recovery when adding bafilomycin A1 to both compartments on top of 5% BSA in the acceptor, with the exception of the bases quinacrine, fingolimod and amiodarone (Fig. 4). These three compounds showed a Papp increase of about 3- to 5-fold, when adding bafilomycin A1. It was concluded that the addition of BSA to the acceptor compartment already leads to a substantial reduction of cellular Kp for most lysosomally trapped compounds. For lipophilic bases with high cellular binding (V1 recovery < 60%) the addition of bafilomycin A1 can further decrease Kp and increase permeability. It is speculated that lysosomal trapping can affect intestinal absorption of lipophilic bases.[10] Our data show, for compounds like quinacrine, amiodarone or fingolimod this might be the case. On the other hand, unchanged permeability and recovery values were observed for most of the

bases under the V2 assay conditions in the absence or presence of bafilomycin A1, indicating that for most bases lysosomal trapping has a small effect on the rate and extent of absorption (Fig. 4, Supplementary Table S2).

For very lipophilic compounds with predicted logD7.4 values larger than 4, the still incomplete recovery data suggest that the addition of 5% BSA in the acceptor compartment is not sufficient to prevent high cellular binding. Interestingly, increasing the lipophilicity of the acceptor compartment by adding liposomes resulted in substantially higher Papp and recovery values for the two lipophilic compounds amiodarone and NVP200. As expected, the addition of BSA or the maisine oil to the donor compartment resulted in lower permeability of amiodarone. Conversely, the Papp value of NVP200 increased under these conditions. The likely explanation for this different behavior is the formations of micelles by NVP200, indicated by very large difference in FaSSIF compared to buffer pH 6.8 solubility (29 μM versus 0.03 μM). Adding BSA or oil to the donor compartment most likely prevents micelle formation which results in an increased permeability.

The MDCK assay is designed to investigate passive transcellular permeability across a cell monolayer and to provide a first estimation of the fraction absorbed unbiased by other effects impacting absorption as solubility, dissolution, active transport. An integration of all parameters influencing absorption can be achieved e.g. by PBPK modeling. Historical permeability vs. Fa calibration curves included a number of compounds which were (i) substrates of uptake or efflux transporters, (ii) predominant paracellular transported, (iii) solubility-limited absorption (BCS class II and IV), (iv) reported with wrong Fa values. A careful investigation of the initial compound calibration set revealed a number of compounds with the above liabilities, reducing the initial list from 58 to 39 compounds (Supplementary Table S3). An improved correlation between permeability and Fa was observed when using this new compound set together with the MDCK-V2 assay protocol (Fig. 1), which allows a more accurate estimation of Fa. The only outlier identified was erythromycin, for which no mechanistic explanation could be identified yet. For highly lipophilic compounds such as amiodarone low recovery values were still observed with the MDCK-V2 protocol, although the measured permeability matched with the reported fraction absorbed observed in humans. Using a classical transwell assay with a Caco-2 or MDCK cell monolayer does not allow to estimate the paracellular transport contribution as the cell monolayer is tighter than the GI epithelium. Paracellular transport needs to be estimated with other tools. Berben et al. reported that a paracellular component can be mathematically added to the parallel artificial membrane assay (PAMPA), allowing to estimate its potential fractional contribution to total permeability.[17] Therefore, a couple of compounds which are known to be absorbed by paracellular permeation and low transcellular permeability were removed from the list of calibration compounds.

In this study we describe an improved transwell permeability protocol more suitable to cover the physico-chemical property space of today's MedChem efforts which reduces the frequency of molecules under-predicted or annotated undefined due to poor recovery (Supplementary Table S4). The number of compounds classified as high permeable (≥85% Fa) increased from 26% for the V1 assay to 57% for V2 based on recent screening data of molecules in the lead optimization phase at Novartis. The new protocol has been validated with an extended set of reference molecules, including compounds for which the traditional protocol leads to an underestimation of Fa in human. We reviewed all assay parameters that could potentially lead to underestimating permeability of compounds, efflux transport, lysosomal trapping, cellular binding, nonspecific binding in the acceptor compartment of the transwell setup.

In conclusion, the new established MDCK assay delivered higher quality permeability data. Together with the new assay calibration this allows a more precise Fa prediction, especially for larger, more lipophilic compounds beyond the rule of five chemical space.

Appendix A. Supplementary Data

Supplementary data to this article can be found online at https://doi.org/10.1016/j.xphs.2021.01.029.

References

1. Egan WJ, Lauri G. Prediction of intestinal permeability. *Adv Drug Deliv Rev*. 2002;54(3):273-289.
2. Dahlgren D, Roos C, Sjögren E, Lennernäs H. Direct in vivo human intestinal permeability (Peff) determined with different clinical perfusion and intubation methods. *J Pharm Sci*. 2015;104(9):2702-2726.
3. Maubon N, Le Vee M, Fossati L, et al. Analysis of drug transporter expression in human intestinal Caco-2 cells by real-time PCR. *Fund Clin Pharmacol*. 2007;21(6):659-663.
4. Aldrich S MDR1 knockout Caco-2 cells. Available at: https://wwwsigmaaldrichcom/catalog/product/sigma/mtox1001?lang=de&region=CH.
5. Irvine JD, Takahashi L, Lockhart K, et al. MDCK (Madin–Darby canine kidney) cells: a tool for membrane permeability screening. *J Pharm Sci*. 1999;88(1):28-33.
6. Di L, Whitney-Pickett C, Umland JP, et al. Development of a new permeability assay using low-efflux MDCKII cells. *J Pharm Sci*. 2011;100(11):4974-4985.
7. Christopher A, Lipinski FL, Dominy BW, Feeney PJ. Experimental and computational approaches to estimate solubility and permeability in drug discovery and development settings. *Adv Drug Deliv Rev*. 1997;23(1-3):3-25.
8. Bednarczyk D, Sanghvi MV. The impact of assay recovery on the apparent permeability, a function of lysosomal trapping. *Xenobiotica*. 2020;50:753-760.
9. Kazmi F, Hensley T, Pope C, et al. Lysosomal sequestration (trapping) of lipophilic amine (cationic amphiphilic) drugs in immortalized human hepatocytes (Fa2N-4 cells). *Drug Metab Dispos*. 2013;41(4):897-905.
10. Li J, Dong Z, Wu F, et al. Developing a mechanistic absorption model to predict the pharmacokinetics of immediate-release weak base drugs with a long tmax by incorporating lysosomal trapping. *Drug Metabol Pharmacokinet*. 2018;33(1, Supplement):S63-S64.
11. Saha P, Kou JH. Effect of bovine serum albumin on drug permeability estimation across Caco-2 monolayers. *Eur J Pharm Biopharm*. 2002;54(3):319-324.
12. Tavelin S. *New Approaches to Studies of Paracellular Drug Transport in Intestinal Epithelial Cell Monolayers*. Uppsala: Eklundshofs Grafiska; 2003.
13. Adson A, Raub TJ, Burton PS, et al. Quantitative approaches to delineate paracellular diffusion in cultured epithelial cell monolayers. *J Pharm Sci*. 1994;83(11):1529-1536.
14. Sugano K, Takata N, Machida M, Saitoh K, Terada K. Prediction of passive intestinal absorption using bio-mimetic artificial membrane permeation assay and the paracellular pathway model. *Int J Pharm*. 2002;241(2):241-251.
15. Low YW, Blasco F, Vachaspati P. Optimised method to estimate octanol water distribution coefficient (logD) in a high throughput format. *Eur J Pharm Sci*. 2016;92:110-116.
16. Ertl P, Rohde B, Selzer P. Fast calculation of molecular polar surface area as a sum of fragment-based contributions and its application to the prediction of drug transport properties. *J Med Chem*. 2000;43(20):3714-3717.
17. Berben P, Bauer-Brandl A, Brandl M, et al. Drug permeability profiling using cell-free permeation tools: overview and applications. *Eur J Pharm Sci*. 2018;119:219-233.